Laser-induced Tetragonal Periodic Surface Structures Using Circularly-Polarized Laser Pulses

Keisuke Fukuhara[1] and Shigeki Matsuo[*1]

[1]*Shibaura Institute of Technology, 3-7-5 Toyosu, Koto-ku, Tokyo 135-8548, Japan*
[*]*Corresponding author's e-mail: matsuos@shibaura-it.ac.jp*

In this article we report on the fabrication of a tetragonal type of laser-induced periodic surface structure (LIPSS). Circularly-polarized femtosecond laser pulses were irradiated on the surface of stainless steel substrates with uni-orientational scratches. LIPSSs with the tetragonal structure were partly fabricated by optimizing the average laser power. The orientation of the tetragonal structure was determined by the orientation of the scratches. We speculate that the surface scratches play a key role in fabricating the tetragonal structure.

DOI: 10.2961/jlmn.2026.02.2004
Keywords: laser-induced periodic surface structures, LIPSS, circular polarization, femtosecond laser, tetragonal pattern, scratch

1. Introduction

In recent years, laser-induced periodic surface structures (LIPSSs, also called ripples) have been studied extensively [1-3]. LIPSSs can be formed by irradiation with laser pulses on the surface of almost any solid material. The period of LIPSSs is typically as short as or a few times shorter than the wavelength of the laser, thus LIPSSs represent a unique capability in surface nano processing. The applications of LIPSSs include control of optical, friction, and wettability properties [1-5].

Linearly-polarized lasers have been used in most research on LIPSSs. In such cases, a striped LIPSS consisting of ridges and grooves (a one-dimensional [1D] periodic pattern) is usually formed, and the orientation of the ridges and grooves is determined by the orientation of the electric field of the laser. The fabricated periodic structures are usually not perfectly ordered: the ridges and grooves may be slightly curved, and may contain branches. To make highly-ordered LIPSSs, Miyazaki and Miyaji developed a two-step process [6,7]. The first step is to irradiate two femtosecond (fs) laser beams overlapping in space and time, resulting in a regular 1D periodic interference pattern whose period is a few times larger than that of the final LIPSS. The second step is to irradiate a single fs laser beam on the interference pattern, which yields a highly-ordered LIPSS. Also, Kodama *et al.* used a combination method of ultraprecise mechanical machining and laser processing, that is, mechanically cutting regular grooves with a period of 10 or 50 μm, followed by laser irradiation [8]. In addition, the fabrication of LIPSS without branches by precisely choosing the laser and scanning parameters has been reported [9-11].

Besides stripe patterns, linearly-polarized lasers occasionally yield a two dimensional (2D) LIPSS [12-19]. For example, Cong *et al.* conducted two-color irradiation (800 and 400 nm), and fabricated 2D dot array on a molybdenum substrate [15]. In addition, Maragkaki et al used a stripe-patterned substrate, and obtained 2D LIPSSs by irradiation with linearly-polarized pulses [18].

When a circularly-polarized laser is used, 2D LIPSSs (dot array, hole array, or granular structure) are usually fabricated, with a period similar to that of 1D LIPSSs [20-22]. Romano *et al*. [23] and van der Poel *et al*. [24] observed well-ordered hexagonal pattern 2D LIPSS, while most of the 2D LIPPSs lack long-range order. Durbach *et al*. reported that well 2D LIPSSs (hexagonal and tetragonal) of gold nanoparticles were formed when circularly-polarized nanosecond laser pulses were irradiated onto a silicon substrate with a gold thin film formed on it [25]. Miyagawa *et al*. reported that the pattern changed from spiral to dots structures with increasing pulse number [26].

We here report that a 2D LIPSS with tetragonal periodicity can be fabricated using circularly-polarized fs laser pulses. By irradiation with galvanometer-scanned circularly-polarized fs laser pulses, tetragonal LIPSSs were partly formed on stainless steel substrates with uni-orientational scratches on the surface. Gallego *et al*. investigated the formation of LIPSSs on surfaces with uni-orientational roughness, finding that the roughness has a major impact on the regularity of the LIPSSs [27]. In this study, we

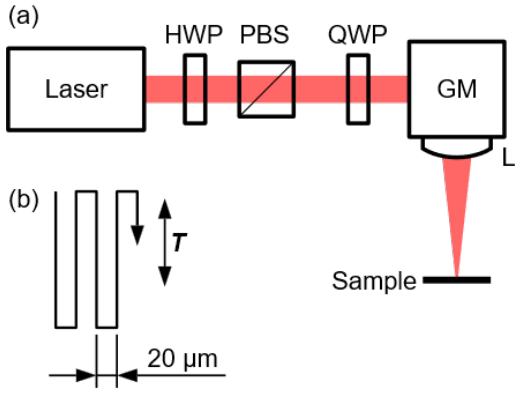

Fig. 1 (a) Schematic representation of the optical setup. HWP: half-wave plate; PBS: polarizing beam splitter; QWP: quarter-wave plate; GM: galvanometer scanner; L: lens. (b) Irradiation trajectory pattern. ***T*** indicates the orientation of the long side of the zig-zag patten.

demonstrate that the scratches also affect the lattice type of the LIPSS.

2. Method

A schematic representation of the optical setup for laser irradiation is shown in Fig. 1(a). The light source used was a Yb:KGW fs laser (Pharos; Light Conversion), which emits linearly-polarized 1030-nm 290-fs pulses at a repetition rate of 10 kHz. The power was controlled using the combination of a half-wave plate and a polarizing beam splitter. Then a quarter-wave plate changed the polarization to circular. The irradiation point of the laser was scanned using a galvanometer scanner (GVS002; Thorlabs) equipped with a scanning lens (LSM04-BB; Thorlabs). The beam diameter at the sample surface was roughly 20 μm ($1/e^2$ intensity). The scanning trajectory pattern was a zig-zag pattern as shown in Fig. 1(b). The orientation of the long side of the zig-zag patten is indicated as ***T***. The distance between adjacent long-side lines was 20 μm. The scanning speed was 50 mm/s, correspondingly the distance between neighboring irradiation points was 5 μm, thus effective pulse number per unit area was about 4.

The sample consisted of substrates of austenitic stainless steel (SUS304 in Japanese Industrial Standards, equivalent to ISO X5CrNi18-10, AISI 304) with a 2B finished surface. The samples were used as supplied. The surface had uni-orientational scratches. The arithmetic mean roughness (Ra) of the samples was approximately 0.07 μm in the orientation perpendicular to the scratches, as measured by a surface roughness tester (SV-2100; Mitsutoyo; tip radius of 2 μm).

The surface of the samples was observed using a scanning electron microscope (SEM) (JSM-IT510LV; JEOL). Fast Fourier Transform (FFT) analysis of the SEM images was performed using ImageJ Fiji [28]. Numerical values of FFT amplitude were extracted from the FFT images.

3. Results and discussion

Figure 2(a) shows a SEM image of the stainless steel substrate before laser irradiation. There are uni-orientational scratches as described in Section 2. Hereafter this orientation is indicated as ***S***. Fourier spectrum of Fig. 2(a) along horizontal axis is shown in Fig. 2(b). The spatial frequency has a blurred peak around 1 μm^{-1} but is widely distributed.

Circularly-polarized fs laser pulses were irradiated on these substrates while scanning the irradiation point. Figures 3(a) and 3(b) show the surfaces after irradiation with an average laser power of 60 mW and 80 mW, respectively. As seen in Fig. 3(a), a LIPSS with a tetragonal pattern was partly fabricated. The period of the tetragonal pattern was approximately 0.95 μm, which is slightly shorter than the laser wavelength. The region of the tetragonal pattern was not large, at a scale of approximately 10×10 dots. This could be expanded by optimizing the experimental parameters. In contrast, a random pattern was fabricated with an average laser power of 80 mW, as seen in Fig. 3(b). This is a typical 2D LIPSS formed with circular polarization. The average laser power of 40 mW resulted in little change; no LIPSS formation was observed. These results indicate that the average power just above the LIPSS formation threshold induces the tetragonal pattern. We speculate that strong irradiation will counteract the substrate's influence, and induce preferential patterns for circular polarization on isotropic substrate, that is, hexagonal-like patterns.

FFT images semi-quantitatively show the difference in LIPSS patterns. FFT images of Figs. 3(a) and 3(b) are shown in Figs. 3(c) and 3(d), respectively. As seen, there are spots reflecting the tetragonal lattice in Fig. 3(c), while only a circle (with a radius corresponding to approximately 0.95 μm period) is seen in Fig. 3(d).

In the case of linearly-polarized light, the orientation of the LIPSS is determined by the orientation of the polarization. However, there is no specific orientation in circularly-polarized light. Therefore, the orientation of the tetragonal pattern must be determined by some other factor. We considered the orientations of scratches ***S*** and scanning ***T*** as potential determining factors. In the images in Fig. 3, however, ***S*** and ***T*** were parallel to each other and it was therefore impossible to determine which was the determining factor. To solve this problem, we performed experiments

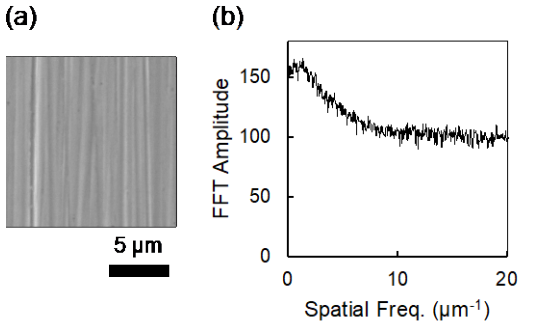

Fig. 2 (a) SEM images of the sample surface before laser irradiation; (b) its FFT spectrum along horizontal axis.

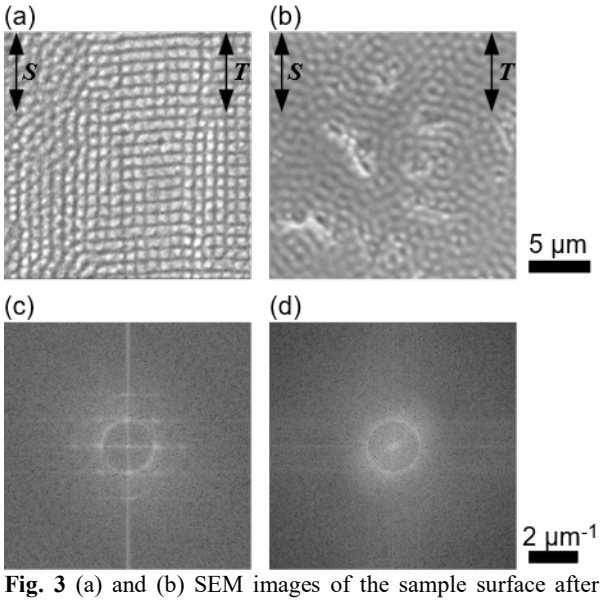

Fig. 3 (a) and (b) SEM images of the sample surface after laser irradiation. The average laser power was 60 mW in (a) and 80 mW in (b). ***S*** indicates the orientation of the scratches, and ***T*** indicates the orientation of the long side of zig-zag pattern of laser scanning. The 5 μm scale bar applies to both (a) and (b). (c) and (d): FFT images of (a) and (b), respectively. FFT was performed on the full images, and half of each obtained FFT image was cropped. The 2 μm^{-1} scale bar applies to both (c) and (d).

with ***S*** and ***T*** at different angles. Figures 4(a) and 4(b) show the results. When the angle between ***S*** and ***T*** was 45° (Fig. 4(a)), a LIPSS with a tetragonal pattern was partly formed, and one of the tetragonal lattice lines was parallel to ***S***, and not to ***T***, indicating that the orientation of the tetragonal pattern was determined by ***S***. It has been observed that sometimes the orientation of LIPSS formed around pre-existing scratches is more affected by the orientation of scratches rather than the orientation of polarization [29]. We speculate that a similar mechanism is at work here so that the orientation of the tetragonal pattern was determined by ***S***. In the case of a 90° angle between ***S*** and ***T*** (Fig. 4(b)), the regularity of the structure was not very good. Figures 4(c) and 4(d) show FFT images of Figs. 4(a) and 4(b), respectively. There are blurred spots corresponding to the tetragonal lattice in Fig. 4(c), but there are no such spots in Fig. 4(d). These results suggest that scanning orientation ***T*** has an effect on the formed LIPSS.

Durbach et al. have also reported formation of tetragonal LIPSSs [25], and honestly their LIPSSs seem to exhibit better regularity than ours. In their case, the LIPSSs consisted of gold nanoparticles on silicon substrates, which can move on the substrate. They observed that regularity is increased with increasing number of irradiated pulses. In contrast, because we use bulk substrates, the surface morphology is less easily changed compared to surface nanoparticles' positions. This may be the reason that our LIPSSs have lower regularity. Instead, in our method, the orientation of scratches can become a factor determining the orientation of 2D LIPSSs. Regarding the determining factor of the orientation of 2D LIPSSs with circular polarization, van der Poel *et al*. supposed that the polarization was not perfectly circular, and the main axis determined the orientation of the hexagonal periodic pattern [24]. In our experiments, when changing the angle between ***S*** and ***T***, the sample was rotated on the sample stage (in other words, the angle of ***S*** with respect to the experimental apparatus was changed), and the other conditions were not changed. Consequently, even if the polarization were elliptical, the relationship between its major axis and ***T*** remains unchanged. Thus, the hypothesis that the lattice orientation is determined by the major axis of elliptical polarization does not agree with our experimental results.

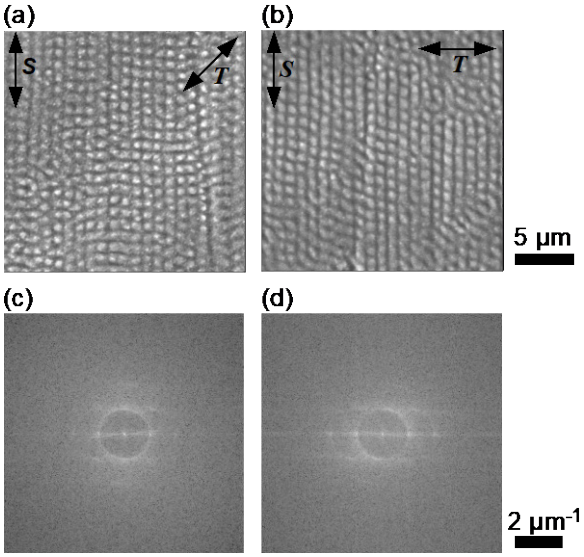

Fig. 4 (a) and (b): SEM images of the sample surface after laser irradiation. The angle between ***S*** and ***T*** was 45° in (a) and 90° in (b). The average laser power was 60 mW. The 5 μm scale bar applies to both (a) and (b). (c) and (d): FFT images of (a) and (b), respectively. FFT was performed on the full images, and half of each obtained FFT image was cropped. The 2 μm^{-1} scale bar applies to both (c) and (d).

As mentioned in Section 1, Maragkaki *et al*. irradiated linearly-polarized laser pulses on a stripe-patterned substrate, and obtained 2D LIPSSs, that is, periodicity in another orientation emerged [18]. They examined this with two orthogonal polarizations, and obtained 2D LIPSSs in both polarizations. Hongo *et al*. found that LIPSSs formed along the pre-existing and randomly-oriented scratches by irradiation with linearly-polarized subnanosecond laser pulses, and the orientation of the LIPSSs was perpendicular to the scratches [30]. These results suggest that there is a mechanism behind periodicity along the ridge or scratch, which merits future clarification.

Given that the orientation of the tetragonal pattern is determined by the orientation of the scratches, the lattice will not necessarily be tetragonal; it may be rectangular (the periods are different in the orientations parallel and perpendicular to ***S***). A systematic examination of experimental parameters may provide keys to controlling the lattice pattern.

4. Conclusion

It was found that LIPSSs with a tetragonal pattern can be fabricated by irradiation with circularly-polarized fs laser pulses. Tetragonal LIPSSs were fabricated on the surface of stainless steel substrates, where uni-orientational surface scratches existed before laser irradiation. The period of the tetragonal lattice was slightly shorter than the laser wavelength. In addition, tetragonal patterns were fabricated with an average laser power just above the LIPSS formation threshold; when the average laser power was increased, the tetragonal structure disappeared, and a random structure emerged. Surface scratches play a key role in the formation and orientation determination of tetragonal LIPSSs.

Acknowledgments

The authors would like to thank Professor Sawa (Shibaura Institute of Technology) for the use of the surface roughness tester.

References

[1] J. Bonse, S. Hohm, S. V. Kirner, A. Rosenfeld, and J. Kruger: IEEE J. Sel. Top. Quantum Electron., 23, (2017) 9000615.
[2] R. Buividas, M. Mikutis, and S. Juodkazis: Prog. Quantum Electron., 38, (2014) 119.
[3] J. Bonse and S. Gräf: Laser Photon. Rev., 14, (2020) 2000215.
[4] J. Bonse: Nanomater., 10, (2020) 1950.
[5] L. Rathmann, T. Rusche, H. Hasselbruch, A. Mehner, and T. Radel: Appl. Surf. Sci., 584, (2022) 152654.
[6] K. Miyazaki and G. Miyaji: J. Appl. Phys., 114, (2013) 153108.

[7] G. Miyaji and K. Miyazaki: Opt. Express, 24, (2016) 4648.
[8] S. Kodama, S. Suzuki, K. Hayashibe, K. Shimada, M. Mizutani, and T. Kuriyagawa: Precis. Eng., 55, (2019) 433.
[9] D. Puerto, M. Garcia-Lechuga, J. Hernandez-Rueda, A. Garcia-Leis, S. Sanchez-Cortes, J. Solis, and J. Siegel: Nanotechnology, 27, (2016) 265602.
[10] K. Bronnikov, S. Gladkikh, E. Mitsai, E. Modin, A. Zhizhchenko, S. Babin, A. Kuchmizhak, and A. Dostovalov: Opt. Laser Technol., 69, (2024) 110049.
[11] Y. C. Liang, Y. E. Li, Y. H. Liu, J. F. Kuo, C. W. Cheng, and A. C. Lee: Opt. Laser Technol., 163, (2023) 109437.
[12] N. Khadka, B. Santa, Y. Yang, A. Ponnuchamy, M. R. Rosenberger, A. J. Hoffman, and E. Kinzel: Opt. Mater. Express, 15, (2025) 2093.
[13] S. Watanabe, Y. Yoshida, S. Kayashima, S. Yatsu, M. Kawai, and T. Kato: J. Appl. Phys., 108, (2010) 103510.
[14] T. Tomita, R. Kumai, H. Nomura, S. Matsuo, S. Hashimoto, K. Morita, and T. Isu: Appl. Phys. A, 105, (2011) 89.
[15] J. Cong, J. Yang, B. Zhao, and X. Xu: Opt. Express, 23, (2015) 005357.
[16] Y. H. Liu, S. C. Yeh, and C. W. Cheng: Nanomater., 10, (2020) 1820.
[17] T. Kobayashi and J. Yan: Nanomanuf. Metrol., 3, (2020) 105.
[18] S. Maragkaki, P. C. Lingos, G. D. Tsibidis, G. Deligeorgis, and E. Stratakis: Molecules, 26, (2021) 7330.
[19] R. Kato and S. Matsuo: Appl. Phys. Express, 16, (2023) 082002.
[20] N. Yasumaru, K. Miyazaki, and J. Kiuchi: Appl. Phys. A, 76, (2003) 983.
[21] J. Reif, O. Varlamova, and F. Costache: Appl. Phys. A, 92, (2008) 1019.
[22] A. Karlash, A. Dmytruk, I. Dmitruk, N. Berezovska, Y. Hrabovskyi, and I. Blonskyi: Appl. Nanosci., 12, (2022) 1191.
[23] J. M. Romano, A. Garcia-Giron, P. Penchev, and S. Dimov: Appl. Surf. Sci., 440, (2018) 162.
[24] S. van der Poel, M. Mezera, G. Römer, E. de Vries, and D. Matthews: Lubricants, 7, (2019) 70.
[25] S. Durbach and N. Hampp: Appl. Surf. Sci. 556, (2021) 149803.
[26] R. Miyagawa, H. Matsuura, A. Nakamura, and O. Eryu: Jpn. J. Appl. Phys., 61, (2022) SK1003.
[27] D. Gallego, I. Ayerdi, A. Pan, S. M. Olaizola, and A. Rodriguez: Sci. Rep., 15, (2025) 15483.
[28] J. Schindelin, I. Arganda-Carreras, E. Frise, V. Kaynig, M. Longair, T. Pietzsch, S. Preibisch, C. Rueden, S. Saalfeld, B. Schmid, J. Y. Tinevez, D. J. White, V. Hartenstein, K. Eliceiri, P. Tomancak, and A. Cardona: Nat. Methods, 9, (2012) 676.
[29] F. Preusch, S. Rung and R. Hellmann: J. Laser Micro/Nanoeng., 11, (2016), 137.
[30] M. Hongo and S. Matsuo: Appl. Phys. Express, 9, (2016) 062703.

(Received: September 3, 2025, Accepted: March 1, 2026)